

## NUMERICAL SIMULATION OF A VERTICAL SLUG FLOW USING THE FINITE VOLUME METHOD

Souza, Marco Antonio Sampaio Ferraz, marco07@fem.unicamp.br  
Guillermo, Juan Jose Navarro, jjgn2010@gmail.com  
Flora, Bruno Fagundes, brunoflora@fem.unicamp.br

Energy Department – DE, Mechanical Engineering Faculty – FEM, State University of Campinas – UNICAMP, CEP 13083-970, Campinas, SP, Brazil

**Abstract.** Numerical simulations were realized using a computer code developed to solve the system of Reynolds Averaged Navier-Stokes equations that can model the motion of a individual Taylor bubble propagating in vertical column in stagnant liquid and upward liquid flow. The domain was discretized in a structured-grid context and several refinements could be made. The finite volume method was used for the discretized system of differential equation. Initially, the velocity distribution far ahead of the bubble was simulated in stagnant liquid and results were obtained for various distances ahead of bubble. The solutions were compared with experimental data available in literature. One of the cases was used to assess the influence of numerical parameters as mesh refinement. At last, the velocity profiles in front of a bubble in upward flowing liquid at various distances from the bubble tip were simulated and the solutions for the axial and radial velocity components and the variation of the axial velocity along the pipe axis were compared with experimental data.

**Keywords:** slug flow, Taylor bubbles, two-phase flow, finite volume method.

### 1. INTRODUCTION

The use of computational tools in simulations of fluid flow and heat transfer known as Computational Fluid Dynamics (CFD) has reduced the projects that use experimental apparatus in real physical situations. The growing capacity of processing and storage of computers allow a more detailed modeling of the problems and the use of more refined meshes in recent years.

In the oil industry, two-phase gas-liquid flow in pipes often leads to intermittent flow or slug flow (Decarre and Liné, 2006). Slug flow is one of gas-liquid flow regimes occurring inside pipes over a wide range of gas and liquid flow rates. In vertical flow, this pattern is characterized by long bubbles, also called Taylor bubbles, which almost fill the pipe cross-section. Gas-liquid slug flow is highly complex with an unsteady behavior (Barnea and Shemer, 2002).

Gas-liquid slug flow is characterized by large elongated bubbles separated by liquid slugs that may be aerated by small dispersed bubbles (Barnea and Shemer, 2002). This type of flow is found in many practical applications, such as: gas absorption units, nuclear reactors, oil-gas pipelines, steam boilers, heat exchangers and air-lift reactors (Nogueira and Pinto, 2005). A detailed study of the entire flow field around a Taylor bubble is a fundamental step towards a reliable hydrodynamic understanding and simulation of this two-phase pattern (Nogueira and Pinto, 2006). A great amount of research has been devoted to the study of this two-phase flow regime (Moissis and Griffith, 1962); (Nicklin et al., 1962); (Campos and Guedes de Carvalho, 1988). An extensive review of this topic is given by (Fabre and Liné, 1992).

The translational velocities of single elongated bubbles in slug flow were simulated for various flow rates. To model the slug flow we considered several simplifications. The results of the simulations were compared with the measured translational velocities of Taylor bubbles in continuous slug flow.

The motion of a single elongated bubble in a vertical pipe is closely related to the movement of Taylor bubbles in slug flow. The translational velocity of the elongated bubble,  $U_t$ , is affected by two factors: the velocity of the liquid ahead of the bubble cap  $U_L$ , and the buoyancy-induced velocity of the bubble in stagnant liquid, i.e., the drift velocity of the bubble,  $U_0$  (Polonsky and Barnea, 1999). The drift velocity is obtained from following expression:

$$U_0 = k\sqrt{gD} \quad (1)$$

where measurements show that the value of  $k$  is in the range of 0.33-0.36 (Nicklin et al., 1962).

For a Taylor bubble rising in a moving liquid the translational velocity of the bubble is a superposition of its rise velocity in stagnant liquid  $U_0$  and the contribution due to the mean liquid velocity  $U_L$  :

$$U_t = CU_L + U_0 \quad (2)$$

The value of the factor  $C$  in Eq. (2) depends on the velocity profile in the liquid ahead of the bubble, and can be seen as the ratio of the maximum to the mean velocity in the profile. Hence, for turbulent flows,  $C \cong 1.2$ , while for laminar pipe flows,  $C \cong 2$  (Nicklin et al., 1962).

The Fig. (1) shows a sequence of images of a gas-liquid slug flow taken with a camera fast.

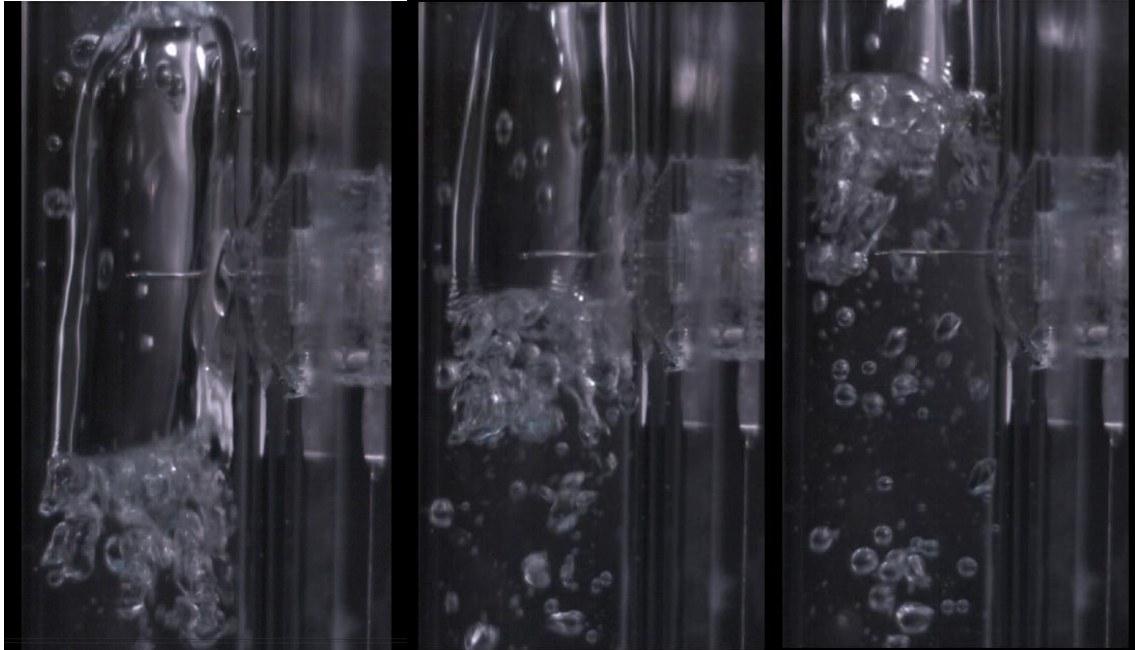


Figure 1. Images of a gas-liquid slug flow. Courtesy Two Phase Flow Group/FEM/UNICAMP.

## 2. THEORETICAL FORMULATION

The fundamental equations of fluid dynamics are:

1. Conservation of mass
2. Conservation of momentum
3. Conservation of energy

Formulations based on non-conservative partial differential equations can lead to numerical difficulties in situations where the coefficients may be discontinuous. Therefore, you must develop the partial differential equations as conservative - or divergent - which has the property that the coefficients are all constant or, if variable, its derivatives do not appear in the equation (Anderson, 1984).

### 2.1 Reynolds Equations for turbulent flow

Although the Navier-Stokes equations model all the physics of the problem to be studied, capture all scales of turbulence that occur in the flow would need computational mesh so fine that would make the numerical solution prohibitive. What is usually done is leave the details and focus on the average values of properties. The result of this process is a system of equations known as Reynolds-averaged Navier–Stokes (RANS) equations (Anderson, 1995).

You can replace each variable by its two parcels in the Navier-Stokes equations and taking the mean of each equation, the resulting system is the Reynolds-averaged Navier–Stokes equations.

Disregarding generating heat and field forces, the conservative form of Navier-Stokes equations using Einstein indicial notation can be written as:

Continuity equation

$$\frac{\partial \bar{\rho}}{\partial t} + \frac{\partial}{\partial x_j} (\bar{\rho} \tilde{u}_j) = 0 \quad (3)$$

Momentum equations

$$\frac{\partial}{\partial t} (\bar{\rho} \tilde{u}_i) + \frac{\partial}{\partial x_j} (\bar{\rho} \tilde{u}_i \tilde{u}_j) = - \frac{\partial \bar{p}}{\partial x_i} + \frac{\partial}{\partial x_j} (\bar{\tau}_{ij} - \overline{\rho u_i'' u_j''}) \quad (4)$$

Energy equation

$$\frac{\partial \bar{e}}{\partial t} + \frac{\partial}{\partial x_j} [(\bar{e} + \bar{p}) \tilde{u}_j] = \frac{\partial}{\partial x_j} \left[ \tilde{u}_i (\bar{\tau}_{ij} - \overline{\rho u_i'' u_j''}) + u_i'' \left( \bar{\tau}_{ij} - \frac{\overline{\rho u_i'' u_j''}}{2} \right) \right] - \frac{\partial \bar{q}_j}{\partial x_j} - \frac{\partial}{\partial x_j} (\overline{\rho u_j'' h}) \quad (5)$$

Compared to the Navier-Stokes equations in the original form, the new terms that appear, are the influence of turbulent fluctuations on the mean flow.

Therefore, it is necessary to shape the new terms to close the system of equations. Most models of turbulence based on the concept of effective viscosity of Boussinesq. The fundamental idea is to add to the molecular viscosity a coefficient of turbulent viscosity as follows:

$$\mu = \mu_l + \mu_t \quad (6)$$

It is assumed that the terms of Reynolds stress can be related to the flow medium in the same way that the tensor of viscous stress is related to the rate of deformation of a Newtonian fluid. You can then write the following relationship

$$\overline{\rho u_i'' u_j''} = \mu_t \left( \frac{\partial \tilde{u}_i}{\partial x_j} + \frac{\partial \tilde{u}_j}{\partial x_i} \right) - \frac{2}{3} \mu_t \frac{\partial \tilde{u}_k}{\partial x_k} \delta_{ij} \quad (7)$$

Similarly, adds to the molecular thermal conductivity a coefficient of turbulent thermal conductivity,

$$k = k_l + k_t \quad (8)$$

The turbulent thermal conductivity,  $k_t$ , is related to the turbulent viscosity, by the relationship:

$$\text{Pr}_t = \frac{c_p \mu_t}{k_t} \quad (9)$$

Where  $\text{Pr}_t$  is the turbulent Prandtl number. The turbulent viscosity,  $\mu_t$ , and turbulent thermal conductivity,  $k_t$ , are not properties of the fluid, unlike the molecular viscosity and thermal conductivity. Dependence of  $\mu_t$  e  $k_t$  on and the flow is the key difficult to model the turbulence. Introducing the hypothesis of Boussinesq, the equations (3), (4) and (5) can be written in terms of average quantities:

$$\frac{\partial \bar{\rho}}{\partial t} + \frac{\partial}{\partial x_j} (\bar{\rho} \tilde{u}_j) = 0 \quad (10)$$

$$\frac{\partial}{\partial t} (\bar{\rho} \tilde{u}_i) + \frac{\partial}{\partial x_j} (\bar{\rho} \tilde{u}_i \tilde{u}_j + \bar{p} \delta_{ij} - \bar{\tau}_{ij}) = 0 \quad (11)$$

$$\frac{\partial \bar{e}}{\partial t} + \frac{\partial}{\partial x_j} [(\bar{e} + \bar{p}) \tilde{u}_j - \bar{\tau}_{ij} \tilde{u}_i + \bar{q}_j] = 0 \quad (12)$$

And the tensor of viscous stresses and the vector of heat flux are now given by:

$$\tilde{\tau}_{ij} = (\mu_l + \mu_t) \left( \frac{\partial \tilde{u}_i}{\partial x_j} + \frac{\partial \tilde{u}_j}{\partial x_i} \right) - \frac{2}{3} (\mu_l + \mu_t) \frac{\partial \tilde{u}_k}{\partial x_k} \delta_{ij} \quad (13)$$

$$\tilde{q}_j = - \left( \frac{c_p \mu_l}{Pr} + \frac{c_p \mu_t}{Pr_t} \right) \frac{\partial \tilde{T}}{\partial x_j} \quad (14)$$

## 2.2 Vector form of equations

Before applying a finite volume algorithm to the fluids dynamics equations it is convenient to write the equations in a compact vector form. Therefore, the Reynolds-averaged Navier–Stokes (RANS) equations, in the conservative form, in two-dimensional Cartesian coordinates, can be written in the following way:

$$\frac{\partial Q}{\partial t} + \frac{\partial E}{\partial x} + \frac{\partial F}{\partial y} = 0 \quad (15)$$

Where  $Q$  is the vector of conserved variables and  $E$  and  $F$  are the vectors of flow in the directions  $x$  and  $y$ , respectively, given by:

$$Q = \begin{Bmatrix} \bar{\rho} \\ \bar{\rho}\tilde{u} \\ \bar{\rho}\tilde{v} \\ \bar{e} \end{Bmatrix} \quad E = \begin{Bmatrix} \bar{\rho}\tilde{u} \\ \bar{\rho}\tilde{u}^2 + \bar{p} - \bar{\tau}_{xx} \\ \bar{\rho}\tilde{u}\tilde{v} - \bar{\tau}_{xy} \\ (\bar{e} + \bar{p})\tilde{u} - \tilde{u}\bar{\tau}_{xx} - \tilde{v}\bar{\tau}_{xy} + \bar{q}_x \end{Bmatrix} \quad F = \begin{Bmatrix} \bar{\rho}\tilde{v} \\ \bar{\rho}\tilde{u}\tilde{v} - \bar{\tau}_{xy} \\ \bar{\rho}\tilde{v}^2 + \bar{p} - \bar{\tau}_{yy} \\ (\bar{e} + \bar{p})\tilde{v} - \tilde{v}\bar{\tau}_{yy} - \tilde{u}\bar{\tau}_{xy} + \bar{q}_y \end{Bmatrix} \quad (16)$$

It is usual to split the flow vector in term of inviscid and viscous parts as follows:

$$E = E_e - E_v \quad \text{and} \quad F = F_e - F_v \quad (17)$$

Where the subscript  $e$  represents the inviscid components for the Euler equations and the subscript  $v$  represents viscous components to be used in the Navier-Stokes equations.

## 3. NUMERICAL IMPLEMENTATION

To obtain the discretization equations from the partial differential equations system, the finite volume method uses the control volume formulation.

We define the vector  $\vec{P}$  as:

$$\vec{P} = E\vec{i}_x + F\vec{i}_y \quad (18)$$

Where  $E$  and  $F$  are the flow vectors defined by equation (16),  $\vec{i}_x$  and  $\vec{i}_y$  are the unit Cartesian vectors. The equation (15) can then be written as:

$$\frac{\partial Q}{\partial t} + \vec{\nabla} \cdot \vec{P} = 0 \quad (19)$$

Integrating the equation (19) for all unit control volumes we obtain :

$$\frac{\partial Q_{i,j}}{\partial t} = - \frac{1}{V_{i,j}} \int_{S_{i,j}} (\vec{P} \cdot \vec{n}) dS \quad (20)$$

Where  $V_{i,j}$  is the volume of a cell and  $S_{i,j}$  is the corresponding control volume surface.

### 3.1 Boundary Conditions

One of the most important tasks of a numerical simulation is the correct implementation of the boundary conditions. Basically, we can define four types of boundaries for the flow which we resolve in this work: solid wall in tube, inlet, outlet and symmetrical boundaries. As it is a two-dimensional case, four conditions at each boundary are necessary to resolve the problem.

### 3.2 Turbulence model of two equations $\kappa$ - $\epsilon$

The  $\kappa$ - $\epsilon$  turbulence model focuses on the mechanisms that affect the turbulent kinetic energy. The standard model (Launder and Spalding, 1974) uses the following transport equations for  $\kappa$  and  $\epsilon$ :

$$\frac{\partial(\rho k)}{\partial t} + \text{div}(\rho k U) = \text{div} \left[ \frac{\mu_t}{\sigma_k} \text{grad} k \right] + 2\mu_t E_{ij} \cdot E_{ij} - \rho \epsilon \quad (21)$$

$$\frac{\partial(\rho \epsilon)}{\partial t} + \text{div}(\rho \epsilon U) = \text{div} \left[ \frac{\mu_t}{\sigma_\epsilon} \text{grad} \epsilon \right] + C_{1\epsilon} \frac{\epsilon}{k} 2\mu_t E_{ij} \cdot E_{ij} - C_{2\epsilon} \rho \frac{\epsilon^2}{k} \quad (22)$$

The equations contain five adjustable constants. The standard  $\kappa$ - $\epsilon$  model employs the following values for the constants for a wide range of turbulent flows:

$$C_\mu = 0.09 \quad \sigma_k = 1.00 \quad \sigma_\epsilon = 1.30 \quad C_{1\epsilon} = 1.44 \quad C_{2\epsilon} = 1.92$$

## 4. RESULTS

### 4.1 Flow field in front of a rising bubble

The problem was solved using a two-dimensional structured mesh containing 180x500 points in the radial and axial directions, respectively. The initial conditions were considered the values of the properties defined as:

$$p = 101325 \text{ N/m}^2 \quad \rho = 998,23 \text{ kg/m}^3 \quad U_L = 0.9 \text{ cm/s} \quad D = 25\text{mm} \quad L = 4\text{m}$$

The boundary condition in wall of the pipe is the condition of non-slipping in the case of the Navier-Stokes formulation. In Fig. (2) a schematic design shows the calculation domain and the boundary conditions. The Fig. (2a) represents the slug flow where the bubble rises with velocity  $U_t$ . The Fig. (2b) shows the condition for the numerical simulation where the bubble is stopped and the wall moves with velocity  $U_t$ .

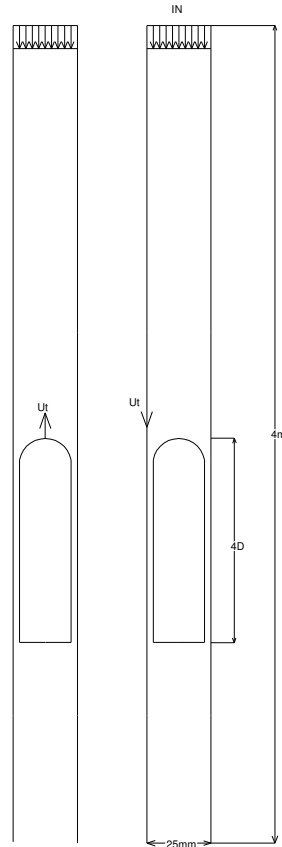


**Figure 2. Schematic design of a Taylor bubble rising. (a) physical problem (b) simulation.**

The translational velocity of the Taylor bubble  $U_t$  can be measured from the displacement of the bubble nose. The drift velocity  $U_0$  can be determined from the measured translational velocity in stagnant liquid in the limit of short bubbles, where the effect of compressibility vanishes (Polonsky and Barnea, 1999). This value is found to be  $U_0 = 17.4 \text{ cm/s}$ , corresponding to  $k = 0.351$ .

The results are compared with experimental data available in Polonsky and Barnea (1999) and showed good agreement. In Fig. (3) are showed the axial velocity profiles at various distances ahead of a 5D long bubble in the pipe cross-section for the upward liquid velocity of  $U_L = 0.9 \text{ cm/s}$ . The red lines represent the results obtained with the numerical simulation and the black lines represent the results presented by Polonsky and Barnea.

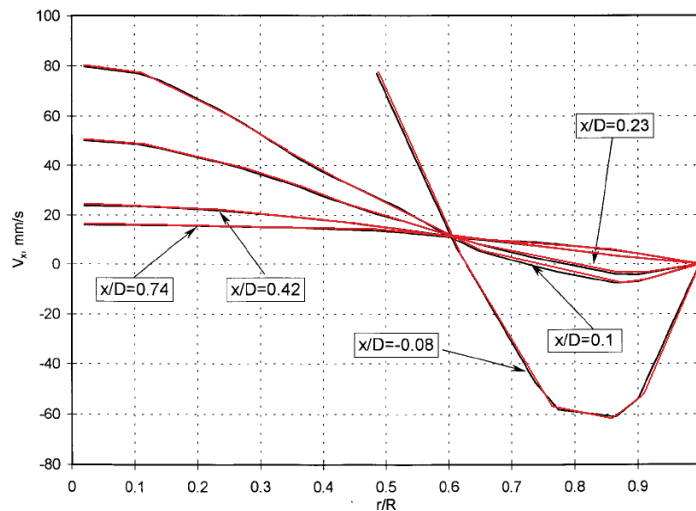


**Figure 3. Axial velocity profiles at various distances ahead of a 5D long bubble,  $U_L = 0.9 \text{ cm/s}$ .**

## 4.2 Velocity components

The velocity profiles in front of a 4D bubble in stagnant liquid at various distances from the bubble tip are showed in Fig. (4) and Fig. (5). In Fig. (4) is plotted the axial velocity component and the results are compared with the experimental results of Polonsky and Barnea (1999). Again, the results of numerical simulation are very close to the experimental data available.

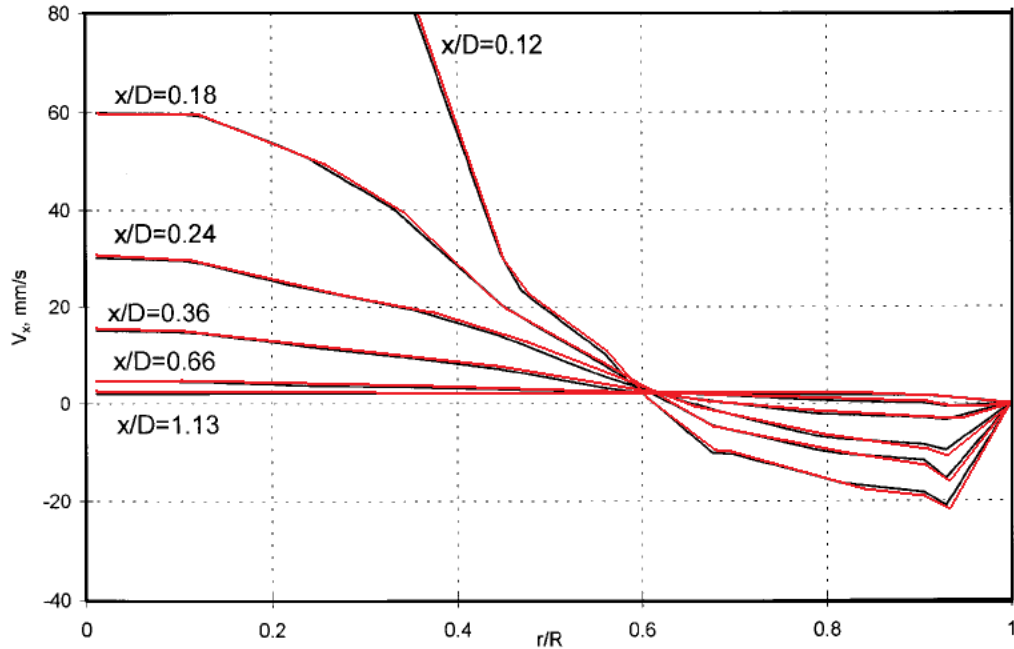


Figure 4. Axial velocity component.

The radial velocity components are showed in Fig. (5) and they also are in good agreement with the experimental data obtained by Polonsky and Barnea (1999).

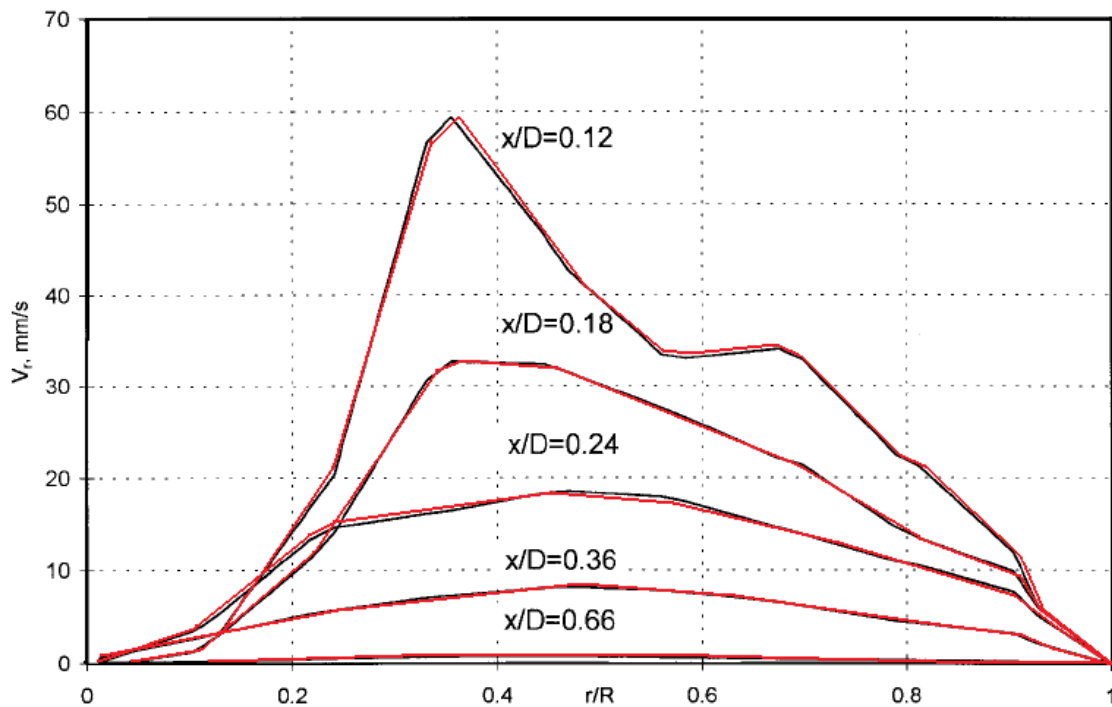


Figure 5. Radial velocity component.



### 4.3 Variation of the axial velocity along the pipe axis

The results of numerical simulation using the finite volume method for the variation of the axial velocity along the pipe axis in upward liquid flow are showed in Fig. (6) and also are in good agreement with the experimental data obtained by Polonsky and Barnea (1999).

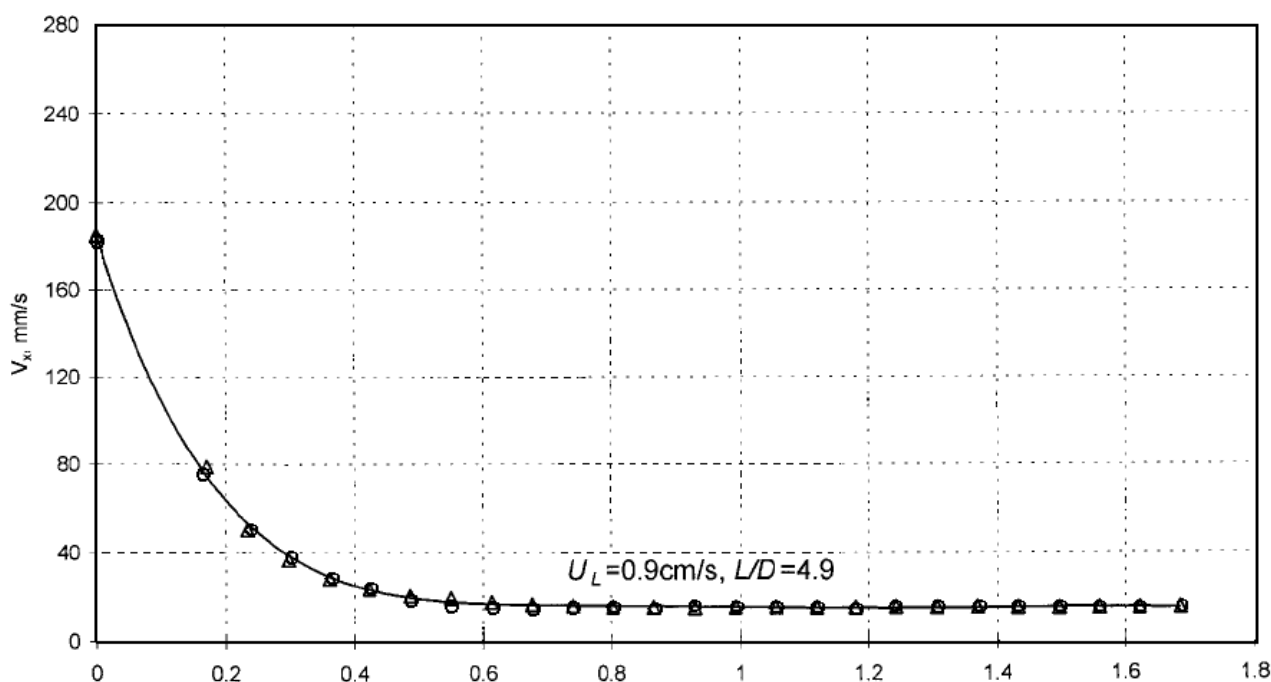


Figure 6. Variation of the axial velocity along the pipe axis.

## 5. CONCLUSION

Numerical simulations involving the hydrodynamic parameters of a single Taylor bubble moving in a vertical pipe in stagnant flow and upward liquid flow were performed. The velocity field in front of a rising bubble, as well as the axial and radial velocity components and the variation of the axial velocity along the pipe axis were simulated using the finite volume method. The solution were compared with experimental data and presenting good agreement. Gas-liquid slug flow is complex and has high costs. Numerical simulations have reduces the steps in projects which use experimental apparatus in real physical situations.

## 6. REFERENCIAS

- Anderson, D. A., Tannehill, J. C., Pletcher, R. H., 1984, *Computational fluid mechanics and heat transfer*, New York: McGraw-Hill.
- Anderson Jr., J. D, 1995, *Computational fluid dynamics: the basics with applications*, New York: McGraw-Hill.
- Campos, J. B. L. M., Guedes de Carvalho, J. R. F., 1988, "An experimental study of the wake of gás slugs rising in liquids, *Journal of Fluid Mechanics* 196, 27-37.
- Fabre, J. Liné, A., 1992, "Modeling of two-phase slug flow". *Annual Review of Fluid Mechanics* 24, 21-46.
- Guet, S., Decarre, S., Henriot, V., Liné, A., 2006, "Void fraction in vertical gás-liquid slug flow: Influence of liquid slug content", *Chemical Engineering Science* 61, 7336-7350.
- Lauder, B.E., Spalding, D.B., 1974, "The numerical computation of turbulent flow", *Comp. Mech. in Appl. Mech. and Eng*, Vol. 3 pp.269.
- Moissis, R., Griffith, P., 1962, "Entrance effects in a two-phase slug flow", *Journal of Heat Transfer* 84, 29-39.
- Nicklin, D. J., Wilkes, J. O., Davidson, J. F., 1962, "Two-phase flow in vertical tubes", *Transactions of the Institution of Chemical Engineers*, 4061-4068.
- Nogueira, S., Riethmuler, M. L., Campos, J. B. L. M., Pinto, A. M. F. R., 2005, "Flow in the nose region and annular filma round a Taylor bubble rising through vertical columns of stagnant and flowing Newtonian liquids", *Chemical Engineering Science* 61, 845-857.
- Nogueira, S., Riethmuler, M. L., Campos, J. B. L. M., Pinto, A. M. F. R., 2006, "Flow patterns in the wake of a Taylor bubble rising through vertical columns of stagnant and flowing Newtonian liquids: An experimental study", *Chemical Engineering Science* 61, 7199-7212.



Polonsky, S., Shemer, L., Barnea, D., 1999, "The relation between the Taylor bubble motion and the velocity field ahead of it", International Journal Multiphase Flow 25, 957-975.

Van Hout, R., Barnea, D., Shemer, L., 2002, "Translational velocities of elongated bubbles in continuous slug flow", International Journal Multiphase Flow 28, 1333-1350.

## **7. RESPONSIBILITY NOTICE**

The authors are the only responsible for the printed material included in this paper.